Draft version June 5, 2015
Preprint typeset using LaTeX style emulateapj v. 12/16/11
efilelof

DOUBLE-LOBED RADIO GALAXIES AND THE INTRAGROUP MEDIUM

Ezekiel Silverstein[1], Michael Anderson[2], and Joel Bregman[1]

(Dated: April 2015)
Draft version June 5, 2015

ABSTRACT

The lobes of FR II double-lobed radio galaxies (DLRG) are bent by ram pressure as the galaxy moves through the intergalactic medium of a galaxy cluster, with the degree of bending depending on the galaxy velocity and the density of the ambient gas. Constraints on the gas density are provided by the amount of bending, which is now measured in uniform samples. We cross-correlate a DLRG catalog with AGNs and three catalogs of galaxies over the range $0 < z < 0.70$, obtaining a sample of 81 DLRGs with degree of lobe bending, along with projected distances and velocity differences relative to the cluster center. DLRGs closest to the cluster center have unbent lobes, probably because these are central galaxies not moving through the cluster. The other galaxies within 2 Mpc of the cluster display bending, with the degree of bending decreasing with radius. The space density of DLRGs decreases as $r^{-1.43}$ within 2 Mpc, slightly flatter than the cluster galaxy distribution.

Keywords: ISM: jets and outflows – galaxies: clusters: intracluster medium – galaxies: groups: general – galaxies: jets, catalogs,

1. INTRODUCTION

Double-lobed radio galaxies (DLRGs) are spectacular sights in the radio sky, and also are scientifically interesting because they connect processes on the ∼AU scale of a galaxy's supermassive black hole (SMBH) to the extragalactic scale (∼tens-hundreds of kpc). Such galaxies are historically divided into two classes (Fanaroff & Riley 1974): the less-luminous FR I galaxies with brighter cores and fainter lobes, and the more-luminous FR II galaxies with brighter lobes and fainter cores. The FR I galaxies also tend to be found in optically luminous galaxies (Ledlow & Owen 1996), typically in brightest cluster galaxies (BCGs), the most luminous galaxies of all (Zirbel 1997). FR II galaxies are also found in denser environments, but preferentially in groups rather than clusters (Zirbel 1997).

Bent-double radio galaxies are a subclass of DLRGs, with the angle between their two lobes bent so that they subtend fewer than 180°. They are even more likely to be found in high-density environments than ordinary DLRGs, and are found with roughly equal probability in clusters and groups; in total, 6% of Abell clusters host a bent-double galaxy (Blanton et al. 2001). Due to this correlation, it is thought that there is a relationship between environment effects and the bending of DLRG lobes.

A possible mechanism for this environmental dependence is ram-pressure experienced by the lobes as the galaxy moves through the intragroup/intracluster medium (Miley et al. 1972; Jaffe & Perola 1973; Jones & Owen 1979). There are other possibilities, however, such as collisions between outflowing lobes and other cluster galaxies (Stocke et al. 1985) or merger-induced precession of the SMBH spin axis (Merritt & Ekers 2002). Each mechanism predicts that more bent DLRGs should arise in dense environments, but there are perhaps second-order observable differences which may be used to distinguish between them (e.g. Rector et al. 1995).

Regardless of which mechanism drives the relationship between bent doubles and environment, a few researchers have begun to invert the relationship, using bent doubles to probe the diffuse gas around the galaxies. Freeland et al. (2008) examined two FR I bent DLRGs, one inside a small group and the other at a projected distance of 2 Mpc from a group, and inferred intergalactic gas densities of 4×10^{-3} cm^{-3} and 9×10^{-4} cm^{-3}, respectively, at the locations of these galaxies (assuming the bending was caused by interaction with diffuse intergalactic gas). Freeland & Wilcots (2011) expanded this analysis to seven bent DLRGs, and found similar results. Finally, Edwards et al. (2010) discovered a bent-double radio galaxy at a projected distance of 3.4 Mpc from the center of Abell 1763, from which they inferred the presence of a cluster filament and provided loose constraints on its density.

Here we extend this type of analysis to a much larger sample of bent DLRGs, using the catalog of DLRGs compiled by de Vries et al. (2006). We cross-match this sample of DLRGs with various catalogs of massive halos (luminous red galaxies, galaxy groups, and galaxy clusters) which collectively span a significant fraction of Cosmic time. With this dataset, we can study the environmental dependence of several properties of DLRGs, including their number density, the angle of the lobes, and the radio luminosity of the lobes. From these measurements, we can constrain the diffuse intergalactic medium in unprecedented detail.

The structure of this paper is as follows. In Section 2, we discuss the catalogs examined in this work, and the various selection criteria which were used to generate them. In Section 3, we discuss the methods used for cross-matching the DLRGs with massive halos, and in Section 4 we analyze the results of this cross-matching in order to measure the environmental behavior of bent doubles. In Section 5 interpret these results and constrain both the mechanism causing the bending and the

[1] Department of Astronomy, University of Michigan, Ann Arbor, MI 48109; ezmasilv@umich.edu, jbregman@umich.edu
[2] Max-Planck Institute for Astrophysics, Garching bei Munchen, Germany; michevan@mpa-garching.mpg.de

large-scale properties of the intergalactic medium.

2. SAMPLE AND METHODS

The primary catalog in this paper comes from De Vries, Becker, and White (2006; hereafter DBW). They cross-matched 44894 quasars from the Sloan Digital Sky Survey (SDSS) Data Release 3 with the Faint Images of the Radio Sky at Twenty centimeters (FIRST; Becker et al. 1994) survey from the Very Large Array (VLA) in order to construct the largest sample of DLRGs. For each SDSS quasar, DBW examined each radio source projected within 450″, using a pairwise ranking system in order to evaluate the probability of the radio sources being lobes of the central quasar. Their ranking system favors potential sources which are closer in the sky to the central quasar and which have larger opening angles.

2.1. *DLRGs*

From the 44894 SDSS quasars, DBW identified 35936 candidate DLRGs. A significant fraction of these candidate DLRGs are "false positives" - quasars for which two radio sources are projected by chance in the sky such that the algorithm of DBW identifies them as potential radio lobes. DBW studied the incidence of these "false positives" and found that, for pairs of radio sources around a quasar with a projected separation of less than 90", a large majority of the candidate DLRGs are real DLRGs (especially for opening angles close to 180°). Candidate DLRGs with projected separations of 60"-120" are about equally likely to be real DLRGs or false positives. Based on these results as well as our own studies of these populations, we select the 780 DLRG candidates with projected lobe separations less than 90" for further study. The remaining 780 candidate DLRGs have redshifts ranging from $z = 0.041$ to $z = 4.889$, and there is no single catalog tracing large-scale structure in SDSS over such a wide range of redshifts. We therefore created a composite sample using three different large-scale structure catalogs spanning different redshifts.

2.2. *Groups and Clusters*

The first bin spans z=0 to z=0.20. This entire volume is covered by a flux-complete (down to Galactic-extinction-corrected Petrosian r-magnitude of 17.77) group and cluster catalog (Tempel et al. 2014) containing 82458 groups and clusters.

At higher redshift it is more difficult to identify groups and clusters using the relatively shallow SDSS photometry. Instead, we use the catalogs from the SDSS-Baryon Oscillation Spectroscopic Survey (BOSS) Data Release 10 (Ahn et al. 2014). BOSS is a spectroscopic survey of massive galaxies in the SDSS footprint. There are two sets of catalogs - LOWZ and CMASS - with slightly different photometric selection criteria. The selection criteria are designed such that both catalogs are approximately stellar-mass limited with typical $\log M*/M_{\odot} = 11.3$ (Parejko et al. 2013; Guo et al. 2013). At these stellar masses, the BOSS galaxies are predominantly red and highly clustered (Guo et al. 2013), so we take them to be reasonably good tracers of large scale structure at these redshifts. We therefore select galaxies from the LOWZ catalog with $0.20 < z < 0.47$ for our second redshift bin, and galaxies from the CMASS catalog with$0.47 < z < 0.70$ for our third redshift bin. We placed cuts at $z = 0.2$, $z = 0.47$ and $z = 0.7$ to ensure there was not any double-counting between different catalogs. These bins contain 209788 and 446158 central galaxies, respectively. Together, our total list of galaxy groups and clusters contain 738404 objects.

Henceforth these objects will be called 'groups' as they are assumed to represent galaxy groups and clusters.

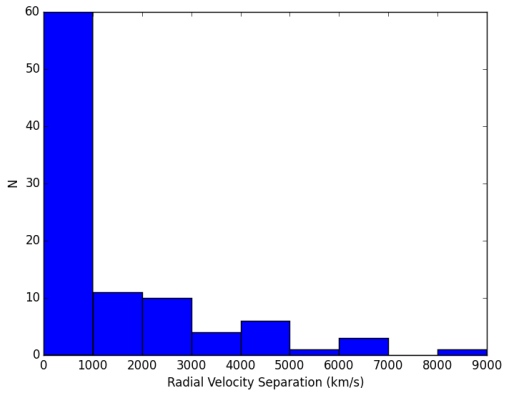

Figure 1. : Histogram of radial velocity separation for the 96 DLRGs with nearest groups within 10Mpc and 10,000km/s. This represents the maximum velocity limit of $\sim 3,000$ km/s that galaxies can have while moving within groups.

2.3. *Cross Matching*

We cross-match the DBW catalog of DLRGs with the large scale structure traces in our various redshift bins. We define a match as a DLRG falling within 10 projected Mpc and 3,000km/s of the trace. We compute the projected distance from the angular separation, assuming the DLRG lies at the proper distance of the tracer, which is computed from the tracer's redshift assuming $\Omega_{\Lambda} = 0.73$ and $\Omega_m = 0.27$. If this projected distance is greater than 10Mpc, or if the difference in recessional velocity between the group and the DLRG is greater than 3,000km/s, we rejected the DLRG-group pair. The limit of 3,000km/s was chosen because it is around the highest velocity a galaxy can have while moving within a group. As seen in Figure 1, there is a steep drop-off of DLRG-group pairs at velocity separations greater than 3,000km/s, supporting our choice of 3,000km/s as the recessional velocity difference cutoff. We found there to be 81 DLRGs with a group within these parameters. This method of cross-matching allows for the possibility of a DLRG matching with multiple galaxy groups. This happens in almost every case (61/81), and when it happens we take the nearest group in terms of projected distance as the only match.

We organized these 81 matches into two sets based on our confidence in their classification as DLRGs. The "Accepted" set is comprised of objects that we are highly confident are in reality DLRGs, while the "Rejected" set holds the remaining objects. A DLRG To do this process, we visually inspected each object, using the VLA FIRST images. Objects that ES, MA and JB all considered real were placed into the Accepted set. DLRGs that were

not deemed to be real were discarded into the Rejected set. Examples of characteristics that caused a DLRG to be discarded included missing 1+ lobes or a clear visible indication that the DWB catalog mistakenly labeled it as a DLRG.

In addition to this manual selection process, we also set certain requirements for the object in order for it to be placed into the Accepted set. First, the sum of the object's central galaxy and its lobes must be brighter than 1×10^{32} erg/s/cm^2/Hz (the specific luminosity separating Fr II objects from FR I objects). 53 of the 81 DLRGs pass this cut while 28 fail. These 28 DLRG-group matches are moved into the Rejected set if not there already.

Second, we require the lobes to be diffuse objects, not point radio sources, so we discard any DLRG if one or both of its lobes appear less than 2.5" in radius. This was done by looking at each object's VLA FIRST image and measuring the diameter of each lobe. 56 of the 81 DLRGs pass this cut while 25 fail, and these 25 are discarded into the Rejected set if not already there.

Third, we require the DLRG to be the brightest radio source within a $1'$ radius region to ensure that the radio lobes are not misidentified as related to the AGN and not related to another object in the region.

To accomplish the second and third cuts, we looked at each object to ensure that the lobes were indeed relatively diffuse and greater than 2.5" in radius, as well as to verify the original lobe placement by DWB. If we disagreed with the DWB lobe placement, we either manually adjusted the lobe's placement, or discarded the DLRG into the Rejected set. We manually changed the lobe placement if it was clear the original placement was incorrect and there was a clear alternative associated with the DLRG core. When there was not a clear alternative, we rejected the DLRG. When a DLRG was placed into the Accepted set yet needed a lobe position update, we repositioned the lobes and recalculated the angle and error of the DLRG using these new coordinates. In most cases the change is small, but for a number of objects we identified one of the lobes with a different radio source than DBW, which caused the bending angle to change significantly. In 13/81 cases the newly calculated angle changed by at least 10°. Of these 13, only 6 were in the Accepted set. Each of these 6 cases is discussed in the Appendix. All objects that fail one or more of these requirements are left in the Rejected set, along with the objects that failed the visual classification. The Accepted set contains 39 DLRG-group matches from the original 81, while the Rejected set contains the remaining 42 matches.

3. RESULTS

3.1. *Distance-Angle Plot*

The primary result of this work is a measurement of the DLRG bending angle as a function of distance to its closest galaxy group. This can be seen in Figure 2. The plots can be understood as segmented into four quadrants, separated by distance of the DLRG to the galaxy group, with a division at 2Mpc and angle of the DLRG lobes, with a division at 170°. We selected a 2Mpc distance between the DLRG and nearest galaxy group as the cutoff between potential DLRG-group association. There appears to be a significant dropoff of bent DLRGs at distances greater than 2Mpc, making 2Mpc a natural division point. It also corresponds to the virial radius of a typical cluster in the sample. We selected a 170° angle cut to differentiate between bent and unbent DLRGs because most objects with angles greater than 170° are consistent with being 180° due to the size of their error bars.

The three DLRGs in the angle range of 125° to 145° and distance from from 6Mpc to 8Mpc are false positives. They may have another galaxy group closer to it that was missed by the group surveys than the one matched with it. At moderate redshifts, the poorer clusters are not identified. These objects can be compared to objects in the same distance range and with angles near 180°, which are assumed to be unbent due to their distance from the group and whose corresponding nearest galaxy group is at the stated distance. The ratio of objects bent below 170° and of objects unbent at distances greater than 2Mpc was used to represent the intergalactic density. This ratio was compared to the ratio of bent against unbent DLRGs within 2Mpc and we found the significance of the different ratios. If there were no difference in the intergalactic medium near the center of the galaxy group compared to further away from it, then the bent-unbent ratios should be similar. As seen in Figure 2, the ratios are not the same, there is a significantly larger ratio of bent-vs.-unbent DLRGs at closer distances and, combined with the known relationship between density and bent DLRGs, it can be inferred that regions of space nearer to centers of groups are denser.

The plot itself contains 39 objects, representing the 39 DLRG-group pairs that passed all of our cuts. There are 6 objects both near a group and not bent below 170°; 7 in the same distance range but bent below 170°; 19 further than 2Mpc from a group and not bent; and 7 further than 2Mpc from a group and bent below 170°. The ratio of bent against unbent within and outside of 2Mpc is 7:6 and 7:19, respectively. Based on Poisson statistics, the probability of this occurring by chance is only 3.85% We also compared the surface density of objects within and outside of 2Mpc. While there are twice as many objects outside of 2Mpc, the surface density of objects inside 2Mpc is much greater, 1.03Mpc^{-2}, compared to that of objects between 2Mpc and 10Mpc, 0.086Mpc^{-2}.

The images in Figure 3 show the 7 objects whose angle is bent below 170° and whose nearest neighboring group is within 2Mpc. The red circles show the location of the DLRG core and lobes, and the red, green and cyan lines from the core to the lobe centers and edges were used to calculate the DLRG angle and errors. These values, along with the distance from the DLRG to its nearest neighboring group, were used to create Figure 2.

3.2. *Control Sample*

To ensure the relationship is between DLRGs and not a peculiar relationship between radio sources, we looked at radio sources that do not pass the lobe angular separation cut of 90". Using the 90" angular separation cut, there is a visible trend that the fraction of bent DLRGs is higher at closer distances. When looking at objects whose lobe angular separation range from 2' to 4', there was not any visible trend. In Figure 4, we see that the distribution is uniform, unaffected by proximity to the galaxy group. This result supports our hypothesis that

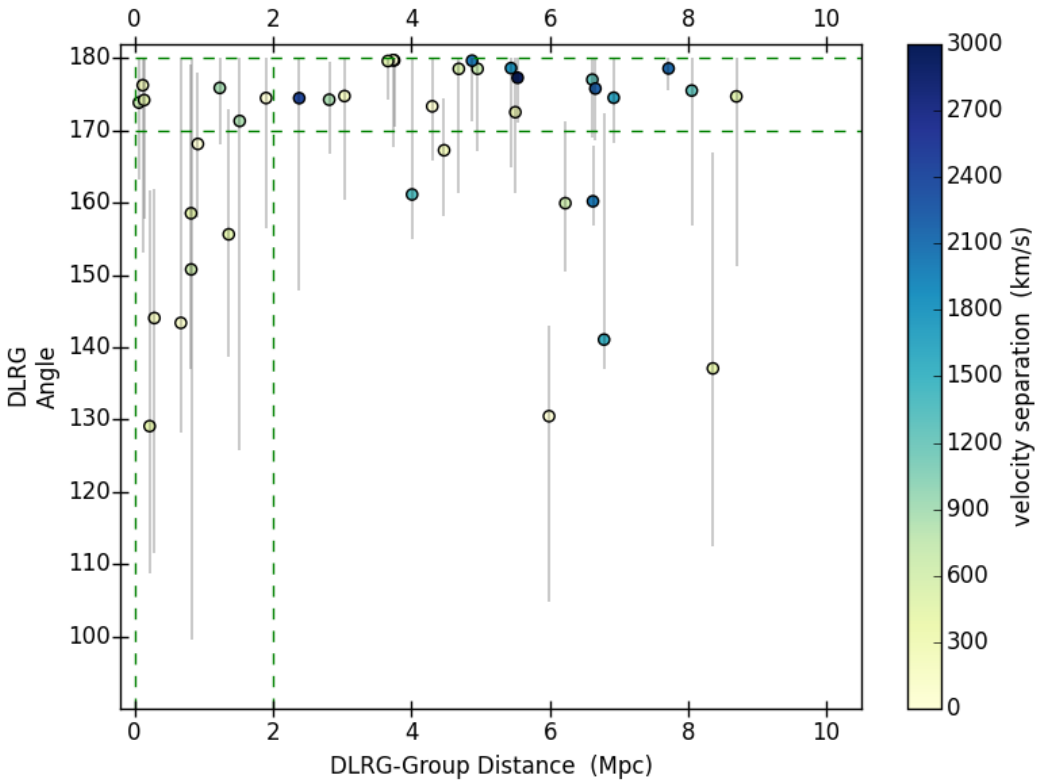

Figure 2. : The angle of the DLRG lobes plotted against the projected distance between the DLRG and its nearest galaxy group. The horizontal dotted line at 170° is the cutoff between "bent" and "unbent" DLRGs. The vertical dotted line at 2Mpc is an approximate separation indicating an environment that influences the bending of the DLRGs. The colorbar on the right-hand side is the velocity separation, or radial distance between the DLRG and its nearest galaxy group. The 39 DLRGs within the Accepted set are shown. Significant bending in DLRGs is uncommon for projected separations exceeding 2Mpc.

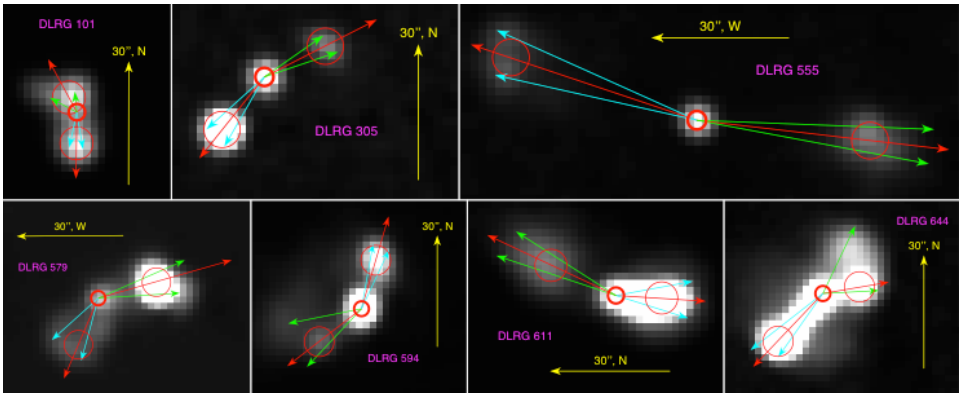

Figure 3. : VLA FIRST images of the 7 DLRGs whose angle is below 170° and whose nearest group is within 2Mpc. The small, thick red circle is the location of the DLRG core and quasar. The larger, thinner red circles are the approximate locations of the DLRG lobes. The lobe positions were located by hand. The red lines from the core through the center of the lobes were used to calculate the angle and the cyan and green lines to calculate the error on the angle. The yellow line shows a 30" length for scale as well as direction for reference. The DLRG number is the object's identification number of the 780 DLRGs with lobe separations less than 90" and matches the identification number in Table **??**.

most objects whose lobe angular separation is less than 90" are connected objects.

4. ANALYSIS

4.1. *Bent vs. Unbent*

To determine the significance of this relationship between DLRG-group distance and DLRG angle, we looked at the relationship compared to the model seen at larger distances. We used binning to measure a ratio at each distance. Using distance increments of 0.1Mpc and bin

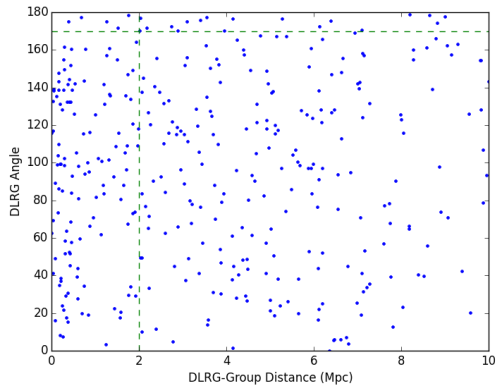

Figure 4. : There are 363 points representing the 363 DBW objects with an angle between their lobes of between 2' and 4'. As in Figure 2, the angle of the DLRG lobes is plotted against the projected distance between the DLRG and its nearest galaxy group. The horizontal dotted line at 170° is the cutoff between "bent" and "unbent" DLRGs. The vertical dotted line at 2Mpc is an approximate radius between environments that influence the bending of the DLRGs.

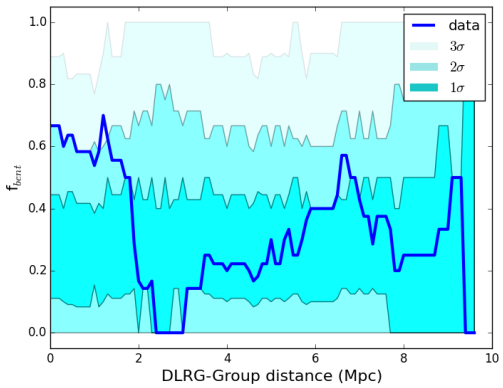

Figure 5. : Confidence intervals around the expected fraction of bent DLRGs at given distances from the galaxy group. The confidence intervals represent the chance that the data is consistent with the model from 2Mpc to 10Mpc where there is no environmental dependence on the angle. We can exclude this occurring by chance at 2σ.

widths of 2Mpc capped by 0 and 10Mpc, we found a ratio of bent and unbent DLRGs in each bin. We also used the model ratio and the total number of galaxies in each bin to find an expected number of bent DLRGs and expected number of unbent DLRGs in each bin. From these expected numbers, we created confidence intervals of 1σ, 2σ, and 3σ and compared it to the actual number of bent and unbent DLRGs in each bin.

Figure 5 illustrates the result. It shows the fraction of bent DLRGs at a given distance as well as the 1σ, 2σ and 3σ intervals around the expected fraction. There is a significant deviation between the observed fraction of bent DLRGs against the expected fraction. The fraction of bent DLRGs is significant to 2σ higher than expected at distances less than 2Mpc, but drops to zero at 3Mpc before increasing again and hovering about the expected value out to 10Mpc. The significance of these deviations at small distances implies that there is a environmental change in the intergalactic space within 2Mpc of the center of galaxy groups.

4.2. *Surface Density*

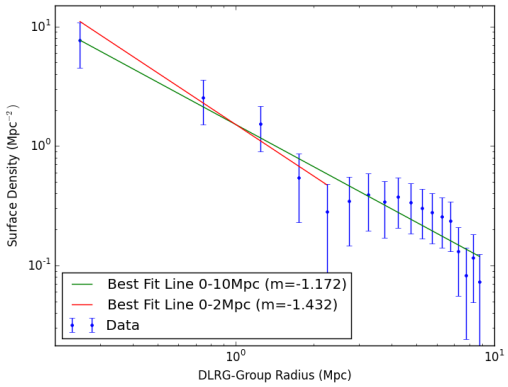

Figure 6. : Plot showing surface density of objects at different DLRG-group radii. The green line is the best fit line for the entire distance range. The red line is the best fit line for distance only up to 2.5Mpc.

We saw in Figure 2 that the surface density of decreased markedly outside of 2Mpc. To examine this further, we bin DLRGs with values starting and ending at 0.25Mpc and 8.75Mpc and increasing 0.5Mpc increments. The bin widths are ±0.5Mpc. The resulting 18 bins cover the radius range from 0 to 9.25Mpc. The largest distance between a DLRG and a group is $\sim$ 8.6Mpc. We then found the surface density of objects within each bin and fit two power-law models to the data, one to the entire distance range and a second to distances only ranging from 0 to 2.5Mpc. It is seen in Figure 6 that the surface density decreases proportional to $r^{-1.2}$, and also that the surface density decreases more rapidly when only small distances are taken into account, proportional to $r^{-1.4}$. An increase of false positive DLRGs can explain the surface density raddecrease at larger distances.

4.3. *Central Galaxies*

In Figure 2, there are three points within 0.15Mpc to the center of their group and above 170°. Additionally, their redshift velocity separations from their respective groups are all below 750km/s. We believe these objects not to be objects in motion about the center of their groups, but in fact the central galaxies. As central galaxies, these objects would be nearly stationary with respect to the group and ram pressure would have a negligible effect on the orientation of their lobes with respect to their cores.

4.4. *Distant Galaxies*

There are another three data points in the region bounded by angles of 125° and 145° and by distances of 6Mpc and 9Mpc of Figure 2. Although it could be the case that these objects are indeed bent and at these large distances away from their respective groups, we believe that there are groups whose intragroup media are

causing this bending, but are too faint to be seen. Supporting this claim is that the redshifts of each of these objects are near the outer limit of their respective redshift catalogs. One has a redshift of z=0.187, near the outer limit of z=0.2 from the Tempel et al. catalog. Another has a redshift of z=0.437, near the outer limit of the LOWZ catalog at z=0.47. The third object has a redshift of z=0.638, near the outer limit of the CMASS catalog at z=0.7. Furthermore, of the 14 objects whose distance to its nearest group is greater than 5Mpc, 11 have redshifts within 0.102 of their respective redshift catalogs' upper limit. This suggests that there may be completeness issues at the outer limits of these catalogs.

5. CONCLUSIONS

We reached our conclusions by cross-matching a DLRG catalog by DWB with a catalog of groups from Tempel et al. and the LOWZ and CMASS catalogs. We set limits on the angular size of the DLRG, the projected physical distance between the DLRG and the group, and the radial velocity separation between the DLRG and the group. We then created plotted angle against distance, Figure 2, and found the relationship between distance and surface density, Figure 6. We found a relationship between distance and fraction of bent DLRGs by creating the confidence interval plot, Figure 5, and the plot of distance against angle for DLRGs, Figure 4, whose angular size was greater than our cutoff and assumed to be three separate radio sources instead of a single DLRG.

We have two primary conclusions. The first conclusion is that there are more DLRGs near the centers of galaxy groups. On the projected sky, there is a significantly greater surface density near the center of galaxy groups, as seen in Figure 6.

The second conclusion is that the fraction of bent DLRGs increases towards the centers of galaxy group centers, supporting our hypothesis. This result leads to the conclusion that the intragroup medium nearer to the center of the group is more dense than the outer regions. This conclusion is reasonable as matter falls towards the galaxy group's gravitational well, increasing the group's density at the center and affecting the orientation of the lobes of DLRGs. Additionally, the change in slope of the two different power-law models, from $r^{-1.432}$ to $r^{-1.172}$, implies the presence of false positive DLRGs at further distances.

Future work on this subject may include finding a direct relationship between distance and DLRG angle or attempting to take into account projection affects and creating a 3D model. Identification of galaxy clusters to a uniform mass level would be of significant benefit to these studies. Further research is required.

Ahn, C. P., Alexandroff, R., Allende Prieto, C., et al. 2014, ApJS, 211, 17

Becker, R. H., White, R. L., & Helfand, D. J. 1994, Astronomical Data Analysis Software and Systems III, 61, 165

Blanton, E. L., Gregg, M. D., Helfand, D. J., Becker, R. H., & Leighly, K. M. 2001, AJ, 121, 2915

de Vries, W. H., Becker, R. H., & White, R. L. 2006, AJ, 131, 666

Edwards, L. O. V., Fadda, D., & Frayer, D. T. 2010, ApJ, 724, L143

Fanaroff, B. L., & Riley, J. M. 1974, MNRAS, 167, 31P

Freeland, E., Cardoso, R. F., & Wilcots, E. 2008, ApJ, 685, 858

Freeland, E., & Wilcots, E. 2011, ApJ, 738, 145

Guo, H., Zehavi, I., Zheng, Z., et al. 2013, ApJ, 767, 122

Jaffe, W. J., & Perola, G. C. 1973, A&A, 26, 423

Jones, T. W., & Owen, F. N. 1979, ApJ, 234, 818

Ledlow, M. J., Owen, F. N. 1996, AJ, 112, 9

Merritt, D., & Ekers, R. D. 2002, Science, 297, 1310

Miley, G. K., Perola, G. C., van der Kruit, P. C., & van der Laan, H. 1972, Nature, 237, 269

Parejko, J. K., Sunayama, T., Padmanabhan, N., et al. 2013, MNRAS, 429, 98

Rector, T. A., Stocke, J. T., & Ellingson, E. 1995, AJ, 110, 1492

Stocke, J. T., Burns, J. O., & Christiansen, W. A. 1985, ApJ, 299, 799

Zirbel, E. L. 1997, ApJ, 476, 489

APPENDIX

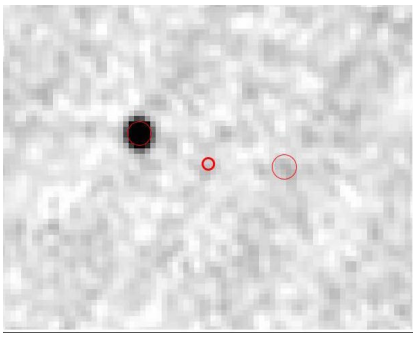

Figure 7. : DLRG 33

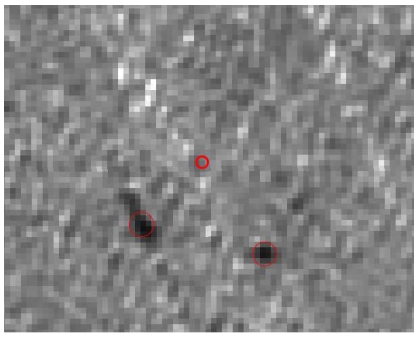

Figure 8. : DLRG 47

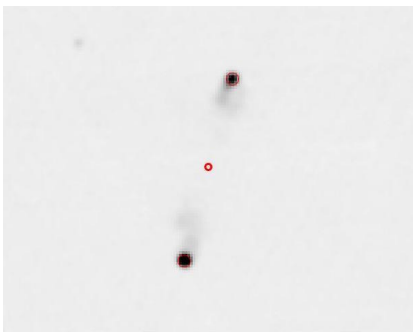

Figure 9. : DLRG 49

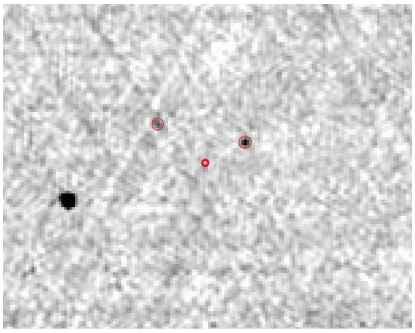

Figure 10. : DLRG 82

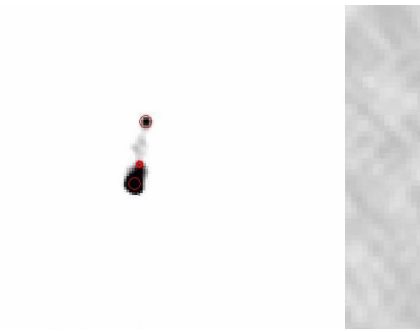

Figure 11. : DLRG 83

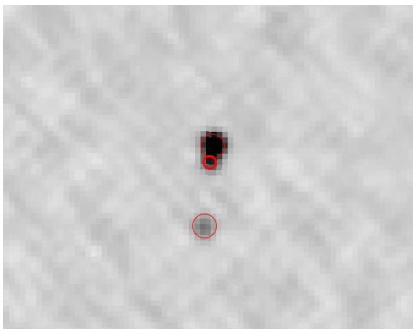

Figure 12. : DLRG 87

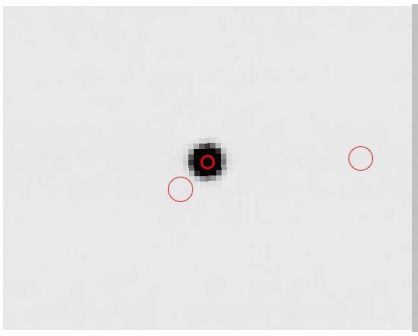

Figure 13. : DLRG 88

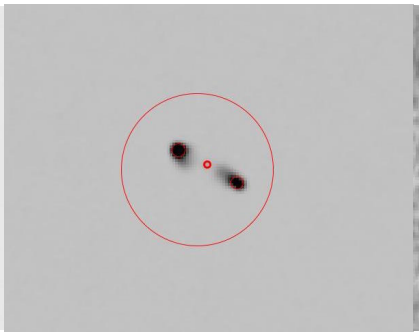

Figure 14. : DLRG 89

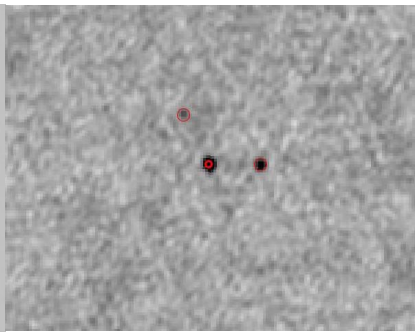

Figure 15. : DLRG 94

Figure 16. : DLRG 101

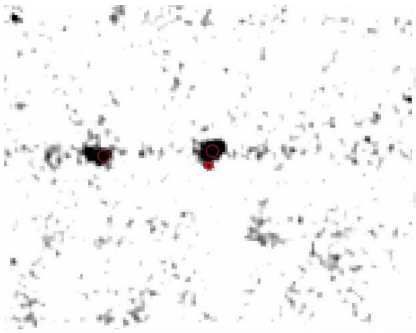

Figure 17. : DLRG 121

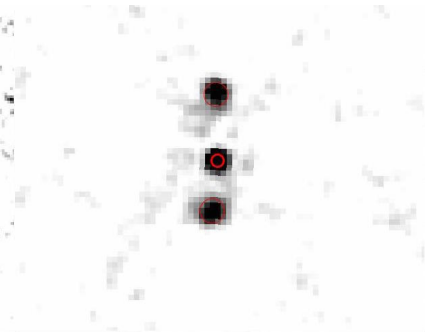

Figure 18. : DLRG 123

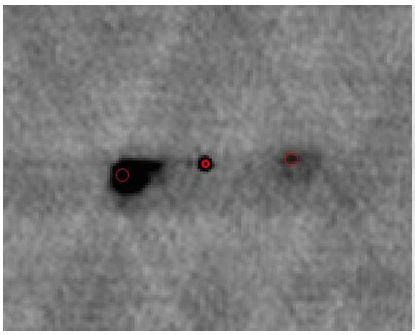

Figure 19. : DLRG 132

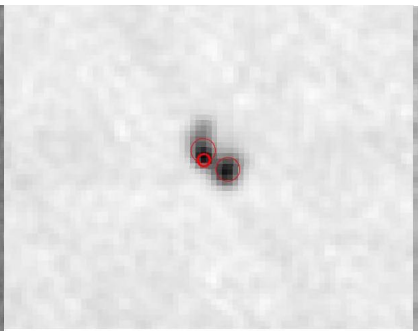

Figure 20. : DLRG 138

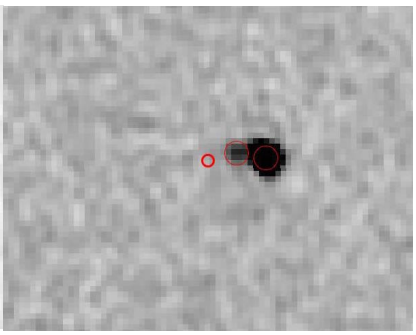

Figure 21. : DLRG 151

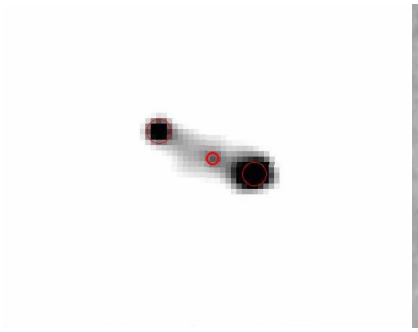

Figure 22. : DLRG 155

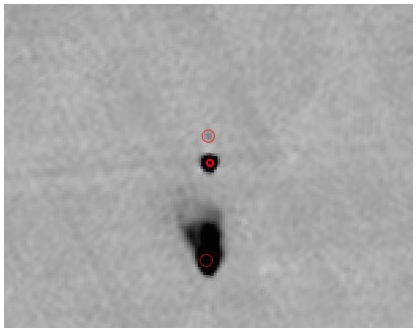

Figure 23. : DLRG 163

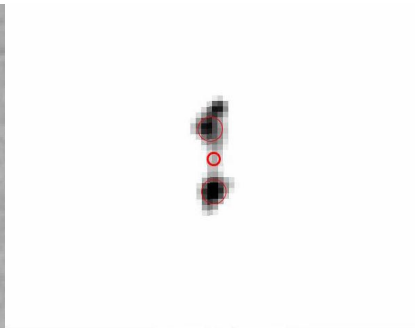

Figure 24. : DLRG 173

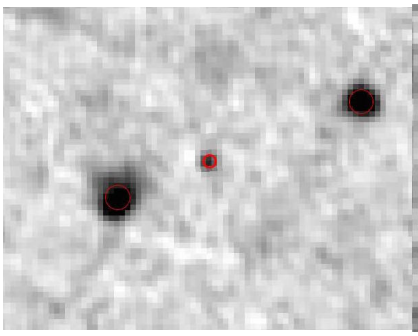

Figure 25. : DLRG 181

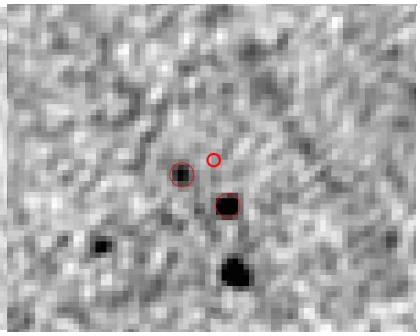

Figure 26. : DLRG 194

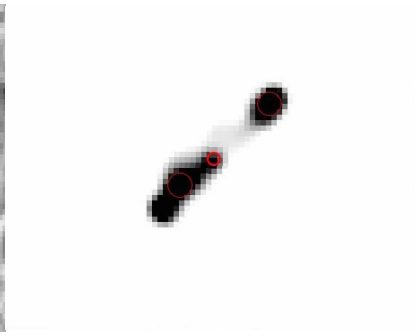

Figure 27. : DLRG 195

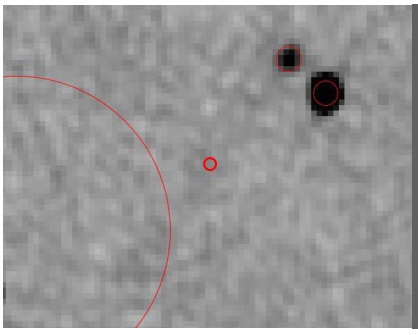

Figure 28. : DLRG 207

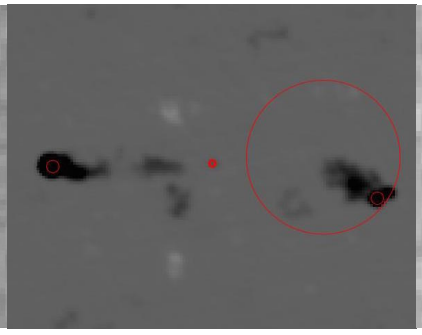

Figure 29. : DLRG 212

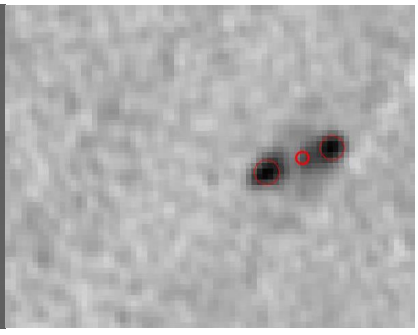

Figure 30. : DLRG 219

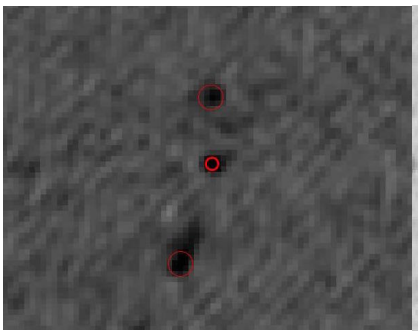

Figure 31. : DLRG 247

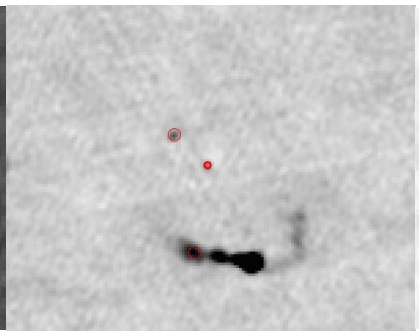

Figure 32. : DLRG 252

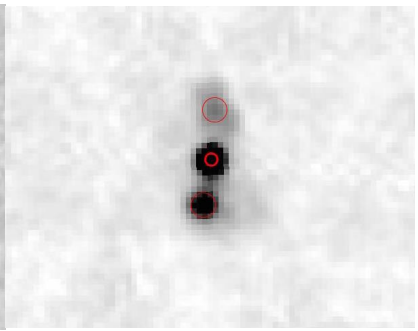

Figure 33. : DLRG 264

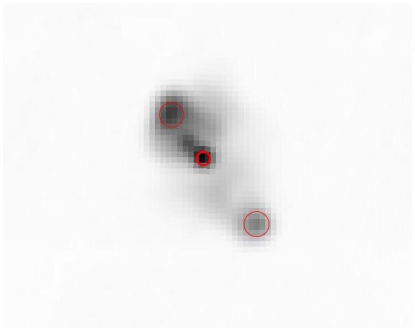

Figure 34. : DLRG 275

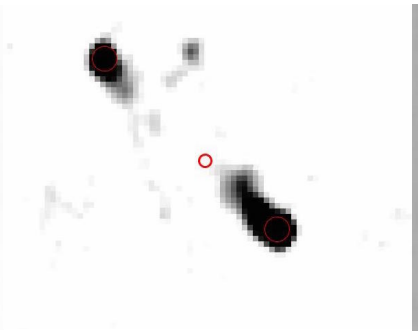

Figure 35. : DLRG 282

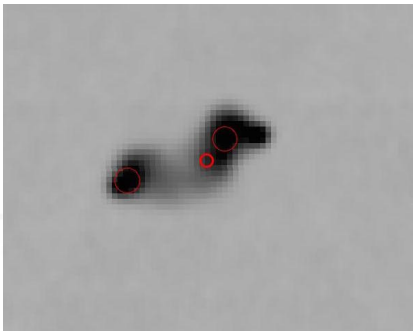

Figure 36. : DLRG 301

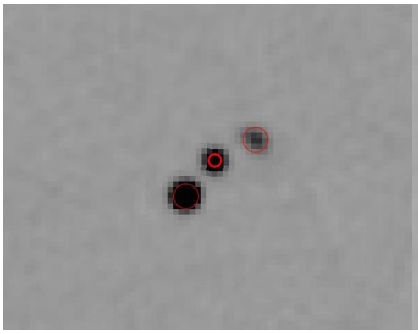

Figure 37. : DLRG 305

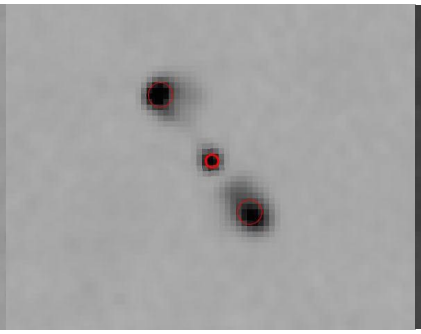

Figure 38. : DLRG 312

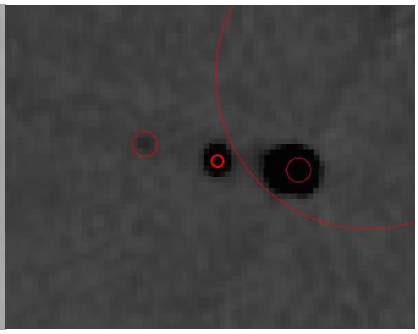

Figure 39. : DLRG 319

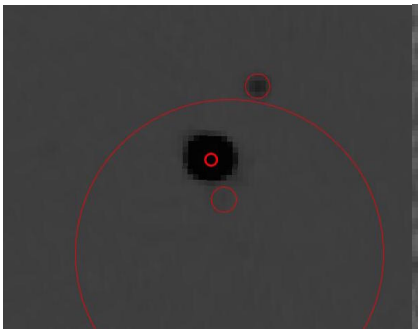

Figure 40. : DLRG 341

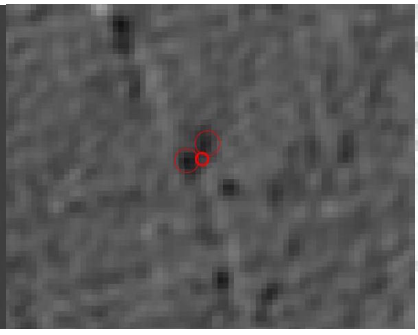

Figure 41. : DLRG 353

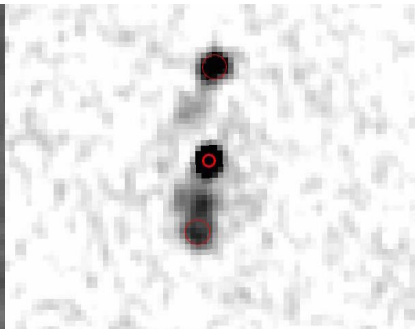

Figure 42. : DLRG 355

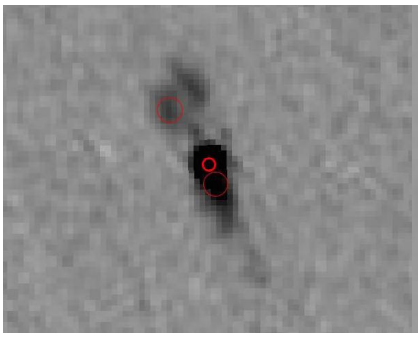

Figure 43. : DLRG 368

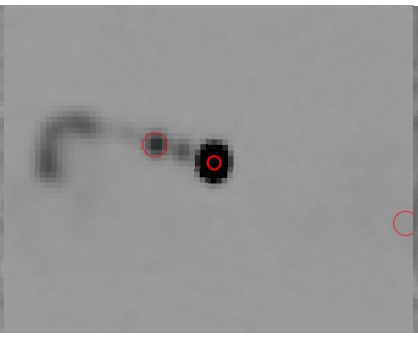

Figure 44. : DLRG 398

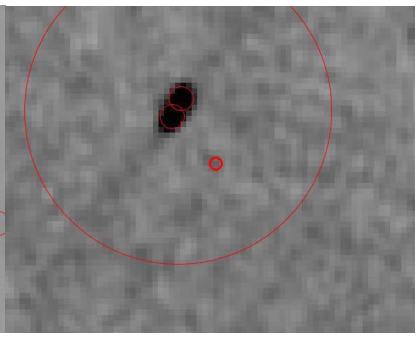

Figure 45. : DLRG 404

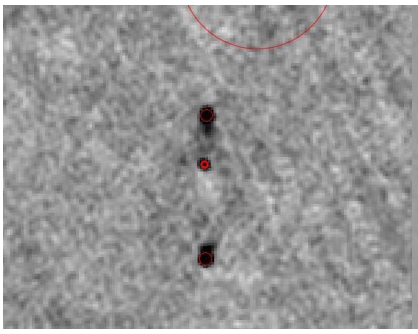

Figure 46. : DLRG 407

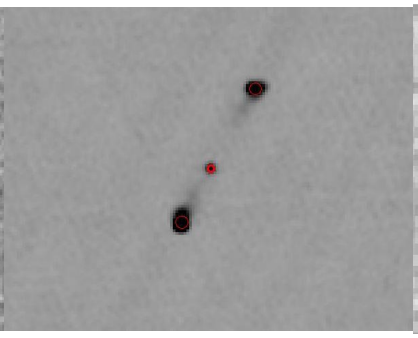

Figure 47. : DLRG 409

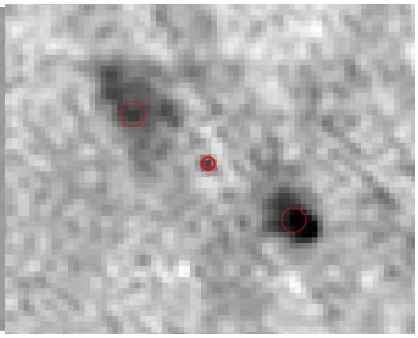

Figure 48. : DLRG 414

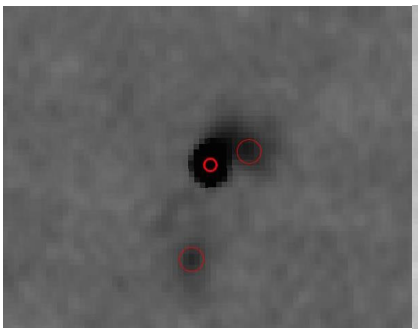

Figure 49. : DLRG 433

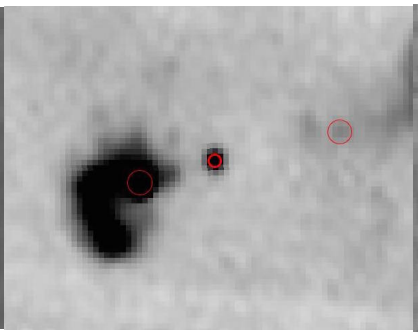

Figure 50. : DLRG 446

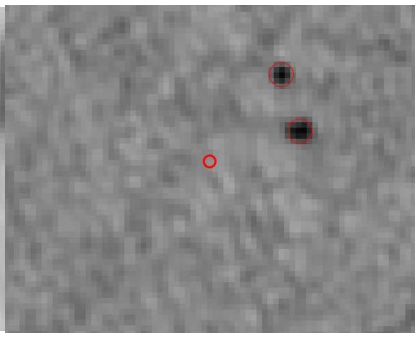

Figure 51. : DLRG 450

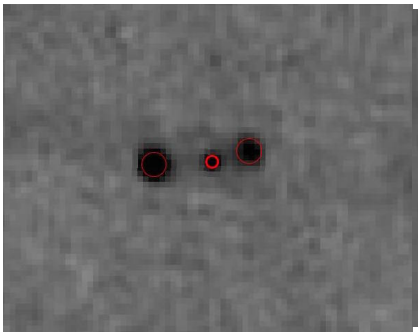

Figure 52. : DLRG 451

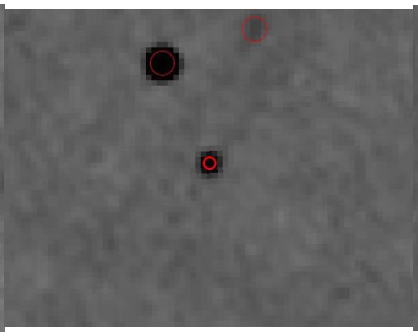

Figure 53. : DLRG 486

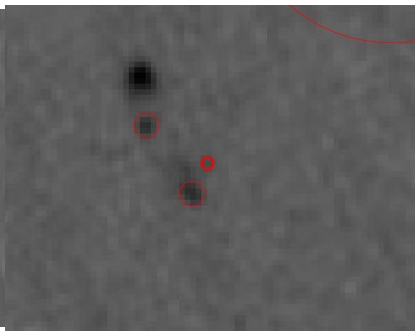

Figure 54. : DLRG 489

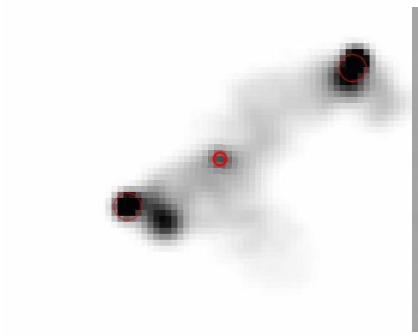

Figure 55. : DLRG 494

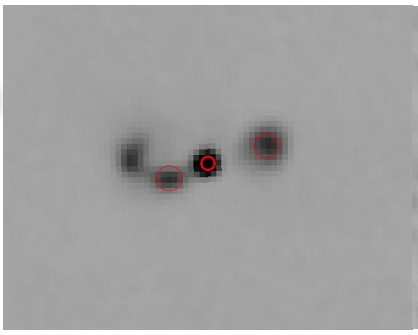

Figure 56. : DLRG 499

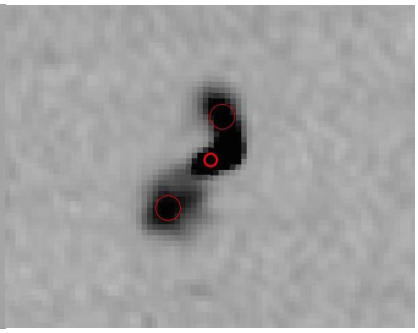

Figure 57. : DLRG 500

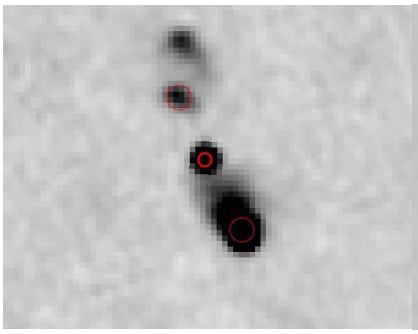

Figure 58. : DLRG 505

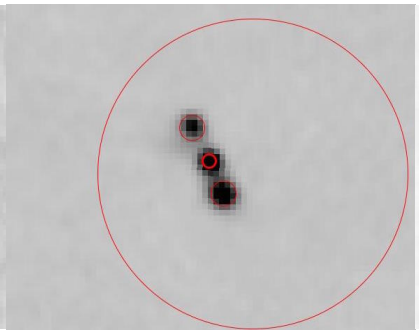

Figure 59. : DLRG 508

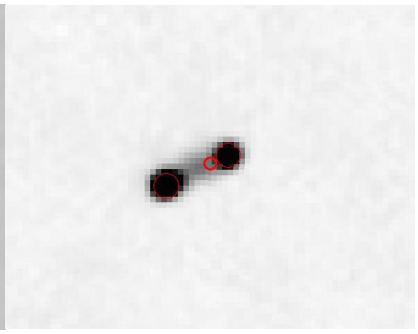

Figure 60. : DLRG 523

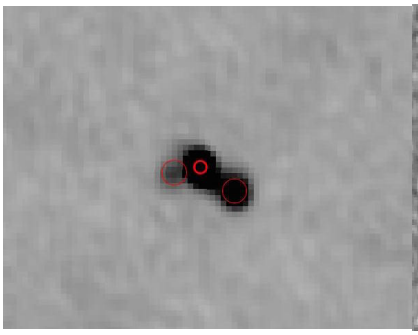

Figure 61. : DLRG 529

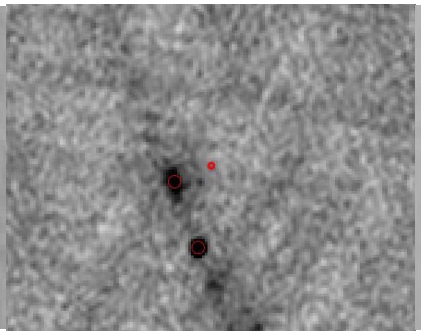

Figure 62. : DLRG 536

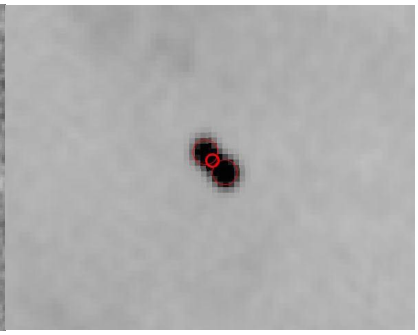

Figure 63. : DLRG 538

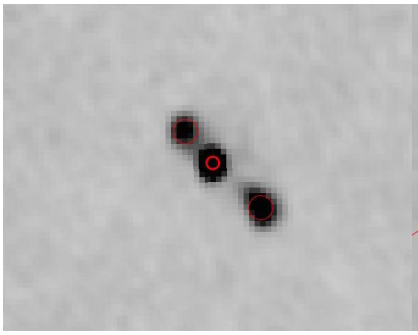

Figure 64. : DLRG 548

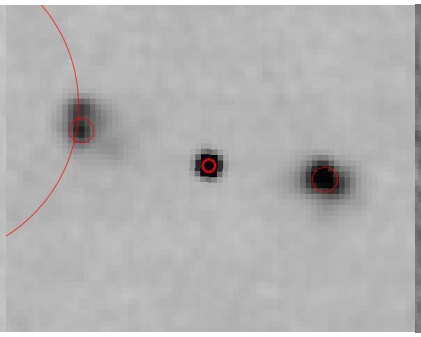

Figure 65. : DLRG 555

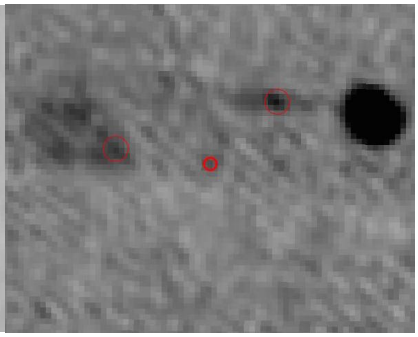

Figure 66. : DLRG 565

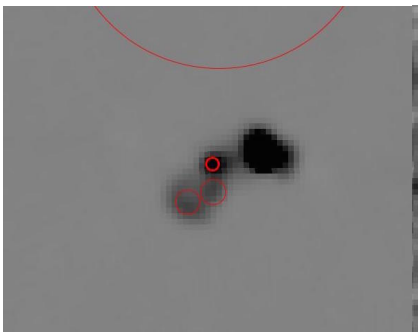

Figure 67. : DLRG 579

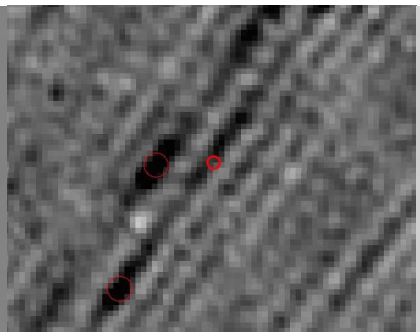

Figure 68. : DLRG 585

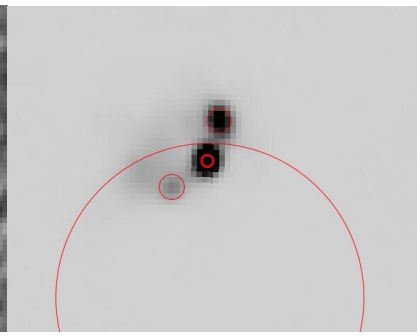

Figure 69. : DLRG 594

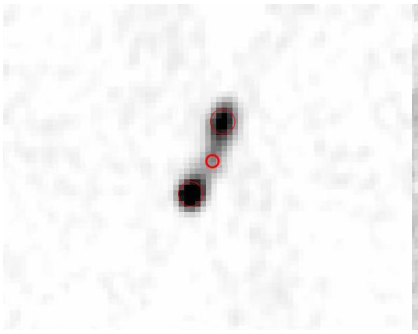

Figure 70. : DLRG 599

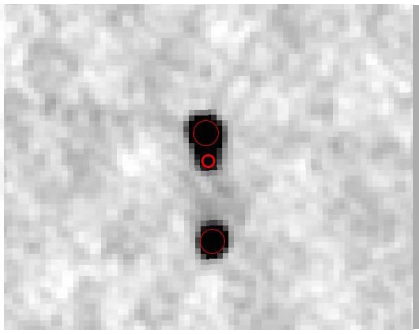

Figure 71. : DLRG 600

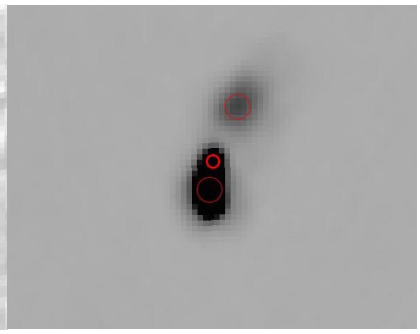

Figure 72. : DLRG 611

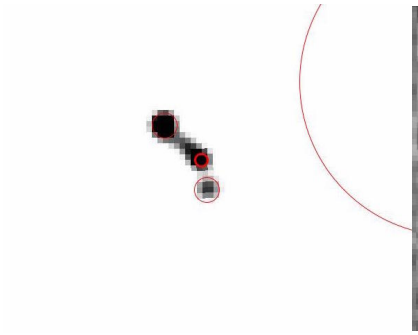

Figure 73. : DLRG 644

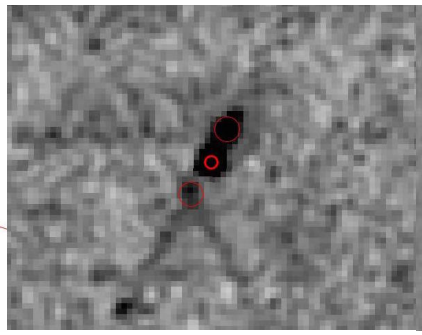

Figure 74. : DLRG 655

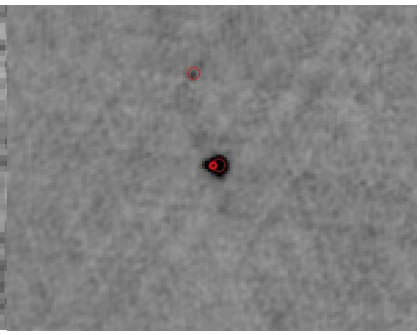

Figure 75. : DLRG 657

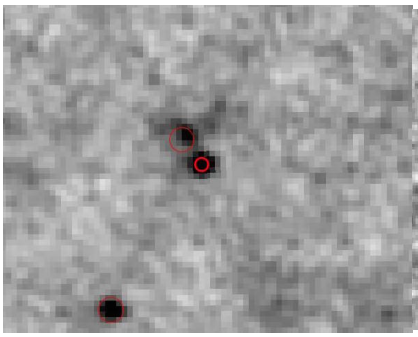

Figure 76. : DLRG 670

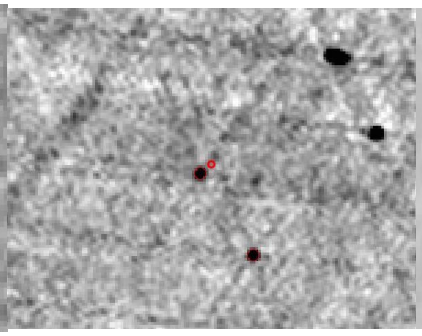

Figure 77. : DLRG 675

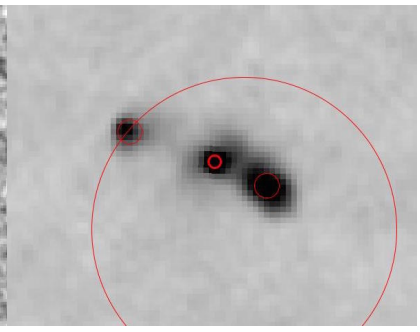

Figure 78. : DLRG 686

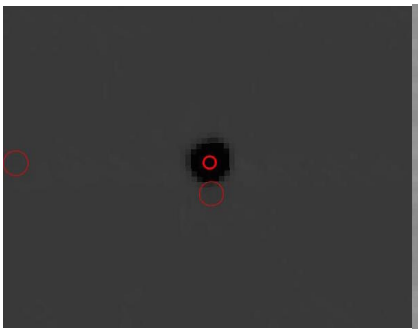

Figure 79. : DLRG 690

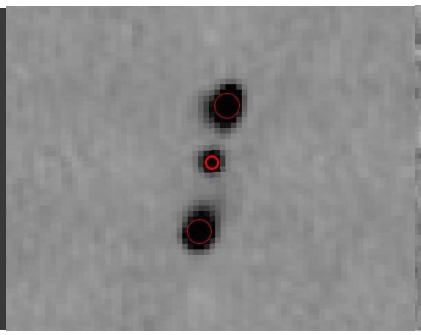

Figure 80. : DLRG 692

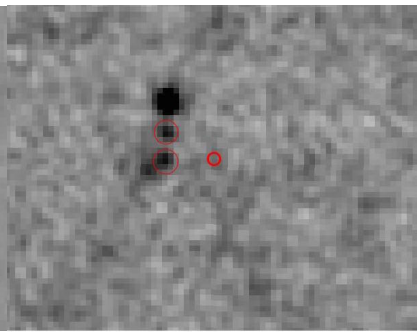

Figure 81. : DLRG 697

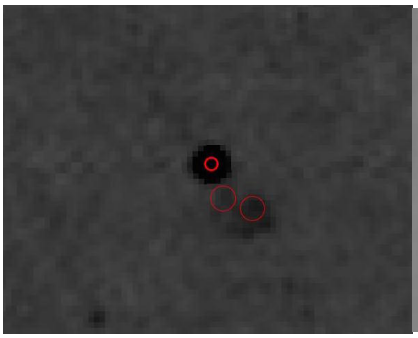

Figure 82. : DLRG 702

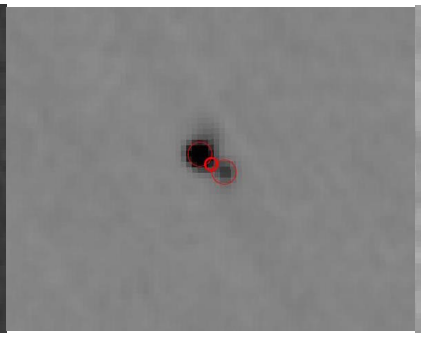

Figure 83. : DLRG 708

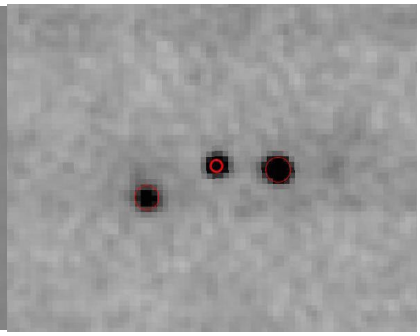

Figure 84. : DLRG 710

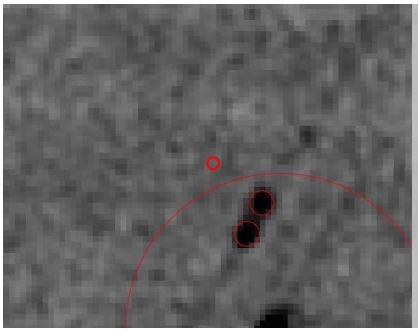

Figure 85. : DLRG 722

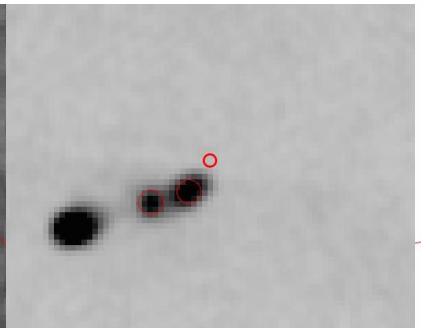

Figure 86. : DLRG 743

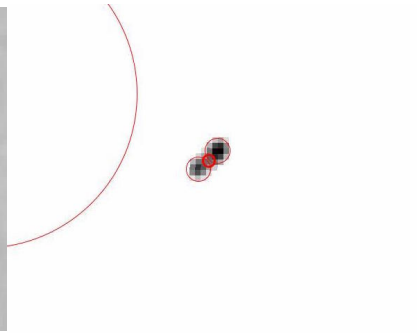

Figure 87. : DLRG 762

Table 1
Data of 81 DLRGs and matched Groups

DLRG	RA (J2000)	Dec (J2000)	Z	Angle (°)	Angle Error (+, -) (°)	Group RA (J2000)	Group Dec (J2000)	Group Z	Set
33	42.6111	0.15094	0.596	158		42.756	0.043	0.59946	Rejected
47	114.9714	31.03914	0.328	78		114.807	31.223	0.33055	Rejected
49	115.35507	33.55558	0.364	179	1, 3	115.524	33.242	0.37118	Accepted
82	122.00729	38.32648	0.041	113		121.305	38.385	0.03587	Rejected
83	122.13905	42.81011	0.543	174	6, 26	122.055	42.86	0.53488	Accepted
87	122.90514	48.52606	0.703	172	8, 11	123.119	48.65	0.69582	Rejected
88	123.2213	40.31664	0.551	136		123.464	40.327	0.55952	Rejected
89	123.32854	50.21106	0.571	174	6, 11	123.331	50.21	0.57335	Accepted
94	124.23421	3.93298	0.404	117		124.226	3.991	0.41013	Rejected
101	125.39003	47.04369	0.128	151	29, 45	125.435	47.133	0.12582	Accepted
121	129.14157	53.01369	0.173	99		129.301	53.336	0.1827	Rejected
123	129.66907	47.56963	0.695	173	7, 12	129.645	47.721	0.69409	Accepted
132	132.66646	54.6315	0.367	174	6, 7	132.466	54.684	0.3641	Accepted
138	134.11633	36.05434	0.345	117		134.491	35.903	0.33808	Rejected
151	136.76169	1.29567	0.571	12		136.721	1.302	0.57008	Rejected
155	137.08757	4.84985	0.524	174	6, 17	137.042	4.804	0.52406	Accepted
163	138.50735	5.13073	0.301	176	4, 7	138.725	5.575	0.30186	Rejected
173	140.60475	43.1304	0.236	172		140.636	42.784	0.2281	Rejected
181	141.90874	1.742	0.419	180	0, 9	141.894	1.893	0.41805	Accepted
194	144.66621	6.46271	0.231	82		144.615	6.167	0.2313	Rejected
195	145.26669	38.8975	0.616	177	3, 6	145.18	38.747	0.62589	Accepted
207	146.21005	2.01507	0.511	179	1, 3	146.357	1.913	0.51641	Rejected
212	146.93811	7.42238	0.086	166	7, 3	146.918	7.424	0.08749	Rejected
219	147.86035	1.78106	0.495	179	1, 14	147.667	1.754	0.48888	Accepted
247	152.25861	7.22885	0.456	160	8, 3	152.035	7.12	0.46281	Accepted
252	153.02314	8.69141	0.095	122	40, 8	153.096	8.69	0.09838	Rejected
264	155.27518	45.39219	0.364	177	3, 8	155.527	45.63	0.36814	Accepted
275	157.9313	52.42644	0.166	179	1, 12	157.554	52.797	0.16837	Accepted
282	159.67511	4.55238	0.423	180	0, 9	159.697	4.361	0.42981	Accepted
301	163.7514	52.03359	0.187	141	31, 4	164.376	51.669	0.19216	Accepted
305	164.22566	5.28702	0.456	156	17, 17	164.174	5.293	0.45756	Accepted
312	166.82867	10.07159	0.633	180	0, 12	166.889	9.978	0.63287	Accepted
319	168.12971	-0.42618	0.544	173		168.108	-0.344	0.53763	Rejected
341	173.24786	10.39505	0.54	130		173.31	10.36	0.5466	Rejected
353	175.83138	3.28641	0.696	170		175.958	3.417	0.69832	Rejected
355	176.29327	1.1823	0.626	175	5, 7	176.498	1.198	0.63159	Accepted
368	178.53867	2.63751	0.211	175	5, 44	178.092	2.504	0.21599	Rejected
398	185.04955	2.06174	0.24	161	19, 6	185.08	1.802	0.2354	Accepted
404	186.64455	3.68081	0.41	15		186.648	3.686	0.41548	Rejected
407	187.64931	9.75526	0.638	176	4, 8	187.64	9.79	0.641	Accepted
409	189.0188	10.58035	0.667	180	0, 6	188.914	10.562	0.66862	Accepted
414	189.81416	53.2374	0.201	170	10, 13	188.962	52.947	0.19353	Rejected
433	193.75201	3.67862	0.437	137	30, 24	194.058	3.565	0.4384	Accepted
446	195.9978	3.65893	0.184	177	3, 29	195.971	3.53	0.18591	Rejected
450	197.15425	0.77784	0.56	32		197.274	0.738	0.55523	Rejected
451	197.17867	2.72409	0.504	167	7, 9	197.178	2.881	0.50315	Accepted
486	204.27888	5.30093	0.163	44		204.246	5.322	0.16457	Rejected
489	204.58318	-2.88079	0.578	95		204.741	-2.965	0.57492	Rejected
494	205.3952	53.74548	0.141	175	5, 15	205.42	53.431	0.1404	Accepted
499	206.439	53.54786	0.135	158	22, 8	206.441	53.381	0.13705	Rejected
500	206.5731	62.34597	0.116	154	26, 15	206.669	62.5	0.11549	Rejected
505	207.72746	5.36847	0.442	175	5, 24	207.814	5.042	0.44039	Accepted
508	208.2731	4.72743	0.523	176	4, 23	208.269	4.726	0.5238	Accepted
523	211.32701	4.56859	0.352	179	1, 18	211.433	4.76	0.35014	Accepted
529	212.37141	-1.95491	0.638	130	13, 25	212.306	-1.791	0.63794	Accepted
536	213.86725	1.11141	0.265	57		213.616	1.057	0.2634	Rejected
538	214.05569	2.31884	0.158	152		214.379	2.478	0.16344	Rejected
548	215.64955	-1.86979	0.666	173	7, 7	215.683	-1.752	0.66582	Accepted
555	216.5258	40.40889	0.664	168	10, 10	216.56	40.414	0.66398	Accepted
565	218.43332	63.96945	0.142	155	12, 21	218.422	64.0	0.14194	Rejected
579	220.76151	52.027	0.141	129	33, 20	220.761	52.05	0.14244	Accepted
585	221.98692	0.55603	0.265	50		221.867	0.394	0.25966	Rejected
594	224.7473	4.27051	0.391	144	18, 32	224.747	4.258	0.39158	Accepted
599	225.34152	1.73368	0.608	160	11, 10	225.213	1.594	0.60576	Accepted
600	226.02129	46.48093	0.632	176	4, 19	226.33	46.37	0.62781	Accepted
611	228.0656	2.05472	0.219	159	20, 22	228.111	2.021	0.22044	Accepted
644	239.32916	45.37266	0.495	143	37, 15	239.297	45.38	0.49533	Accepted
655	242.00008	38.25853	0.464	174		241.714	38.095	0.47375	Rejected
657	243.06274	45.33931	0.502	100		243.166	45.419	0.50278	Rejected
670	246.8895	38.45544	0.367	109		246.888	38.612	0.35779	Rejected
675	247.50143	45.2064	0.399	78		247.598	45.368	0.39831	Rejected
686	249.73557	43.58683	0.339	174	6, 16	249.732	43.581	0.33745	Accepted
690	250.74507	39.81028	0.593	94		250.849	39.892	0.58846	Rejected
692	251.43622	37.92392	0.598	176	4, 7	251.69	37.979	0.5906	Accepted

Table 1 — *Continued*

DLRG	RA (J2000)	Dec (J2000)	Z	Angle (°)	Angle Error (+, -) (°)	Group RA (J2000)	Group Dec (J2000)	Group Z	Set
697	254.15411	37.24433	0.063	32		254.368	36.815	0.06515	Rejected
702	255.30156	35.56483	0.501	24		255.257	35.565	0.49349	Rejected
708	255.89581	39.29323	0.523	171	9, 45	255.957	39.272	0.52014	Accepted
710	256.10464	33.52944	0.29	152		256.053	33.425	0.28917	Rejected
722	259.18161	29.25981	0.544	25		259.281	28.994	0.54513	Rejected
743	325.80826	0.78751	0.493	21		325.696	0.917	0.49627	Rejected
762	346.44028	-0.60239	0.269	171	9, 18	346.461	-0.596	0.26592	Rejected

Note. — List of DLRGs with matched galaxy groups within 10Mpc projected and 3,000km/s radial. The first column is the number the DLRG is out of the 780 candidate DLRGs from the DBW catalog with a projected separation less than 90". The next three columns show the right ascension, declination and redshift of the DLRGs. Columns 5 and 6 show the DLRG's angle and plus/minus. The next three columns are the right ascension, declination and redshift of the DLRG's nearest galaxy group with which it matched. The last column states whether the DLRG was placed into the Accepted or Rejected sets.